

Comparison of Co-located Laser and Metal Oxide Continuous Monitoring Systems

By Kellis Ward^{1,2}, William Daniels^{1,2}, and Dorit Hammerling^{1,2}

¹Department of Applied Mathematics and Statistics, Colorado School of Mines, Golden CO

²Payne Institute for Public Policy, Colorado School of Mines, Golden CO

September 12, 2024

1 Abstract

Accurate measurement of methane (CH₄) concentrations on oil and gas sites is essential for accurate estimates of methane emission rates via inversion algorithms. Different types of continuous monitoring sensors are offered as commercial solutions, with varying accuracy. In this paper we compare data from co-located Metal Oxide (MOx) and Laser Spectroscopy (LS) sensors on a midstream oil and gas site, with the goal of quantifying the differences in raw concentration measurements between the two technologies. We first analyze the impact of meteorological variables on the difference between MOx and LS concentrations measurements taken at the same time and location, finding that temperatures from 30 to 70 degrees Fahrenheit and higher humidity contribute to larger concentration differences on average. Further, analysis of enhanced methane concentrations (likely from emissions on the site) recorded by both sets of sensors reveals that the LS sensors consistently record larger methane concentrations during these periods. This difference means that when using concentration measurements from both sensor technologies in inversion algorithms to estimate emission rates, using MOx sensor data would likely lead to underestimating emission rates, although we did not test this explicitly in this report.

2 Introduction

The accuracy of inverse models for estimating emission rates is predicated on the accuracy of the inputs—methane concentration measurements. Continuous monitoring systems (CMS) are a promising avenue for measuring methane concentrations in near real time on oil and gas sites. There are many different types of CMS that are currently used in practice. Two common sensor technologies are Metal Oxide (MOx) sensors, which measure methane concentrations via changes in resistance across a metal oxide, and Laser Spectroscopy (LS) sensors, which measure methane concentrations using laser absorption. Using two-and-a-half months of methane concentration data from co-located MOx and LS sensors, i.e. sensors on the same pole, we can compare how the different sensor technologies impact methane concentrations measurements recorded at the same location under the same environmental and site operating conditions.

The location used for the study is a midstream site with multiple potential emission sources, of which some emit at a relatively low rate constantly, and others emit only periodically. On this site, a small subset of the potential sources are expected to make up a majority of the total emissions. There are 18 co-located sensors in total placed on the fence line of the site, nine MOx and nine LS sensors. The sensors vary in distance from potential emission sources, and some sensors are expected to record higher concentrations, on average, due to their proximity to potential emission sources and the predominant wind direction on the site. Figure 1 shows an abstracted view of the site.

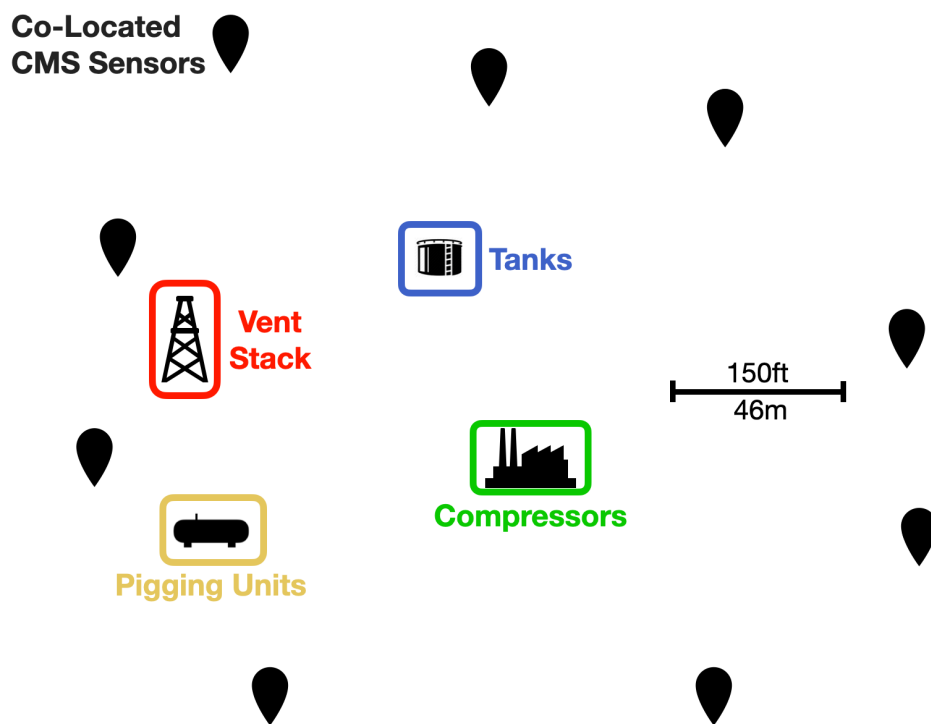


Figure 1: Abstracted site diagram. Major equipment groups are shown and outlined in color, and locations of co-located CMS sensors are shown by black pins.

Figure 2 provides an overview of the concentration measurements from the co-located MOx and LS sensors. The shape of the distributions between the MOx and LS sensors differ greatly. The MOx sensors have very narrow concentration measurement distributions with median concentrations near 2 ppm. The interquartile range (the middle 50% of the data) for each MOx sensor is also very narrow. The LS concentration measurement distributions have varying medians. Most LS sensors record median concentration measurements near 2.5 ppm, however, the

LS-WNW sensor records a larger median concentration measurement than any of the sensors at 2.79 ppm. The interquartile range of each LS sensor distribution is also approximately 1 ppm, much wider than the interquartile range of the MOx sensor distributions, all less than 0.25 ppm. Only the interquartile ranges of the SSW, NW, and ESE LS sensor distributions overlap with the co-located MOx sensor distribution interquartile range.

Distribution of Concentration Measurements, MOx and LS Sensors

Nov. 10, 2023 to Jan. 31, 2024

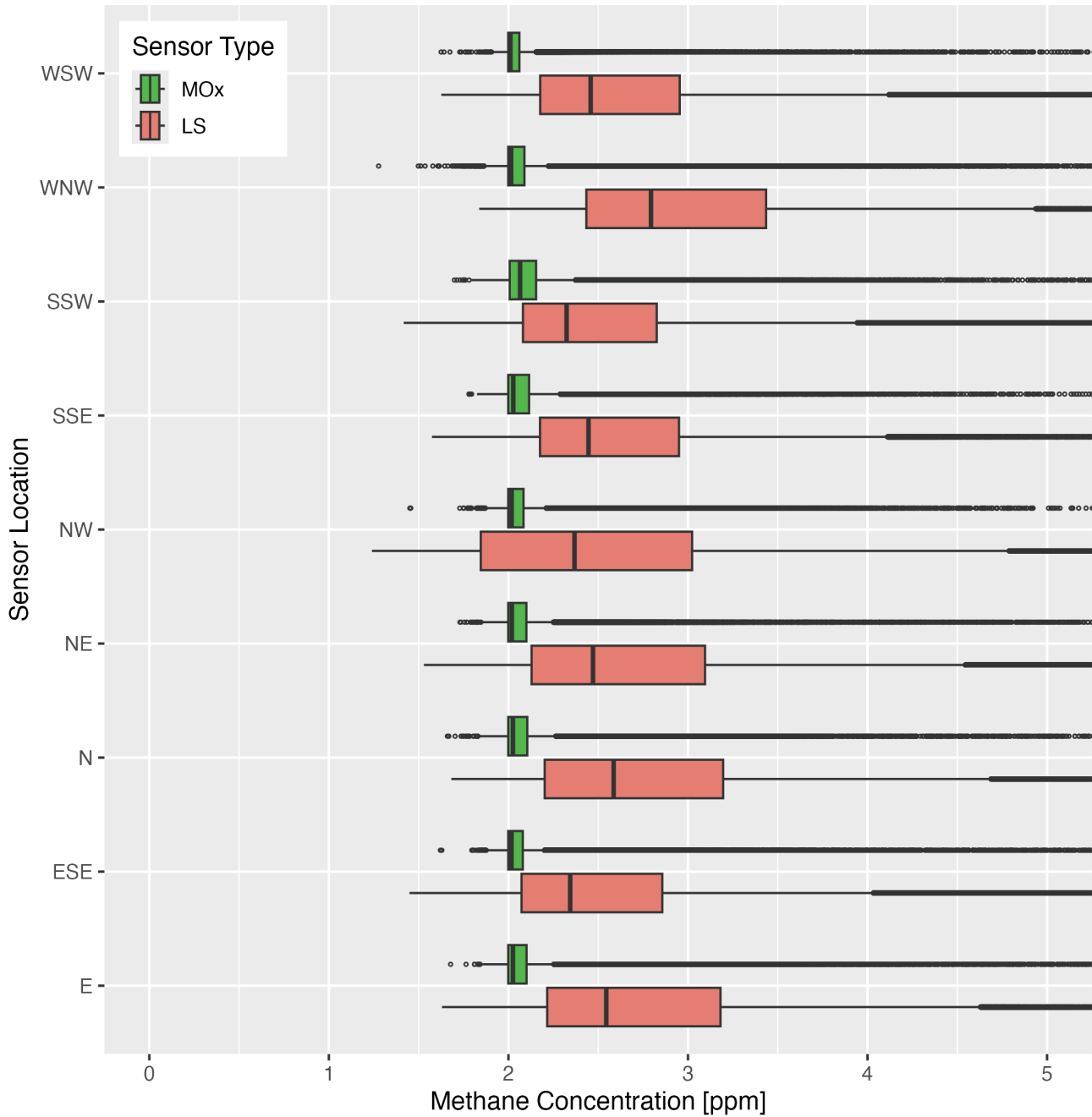


Figure 2: Distribution of concentration measurements grouped by co-located pair location. The green boxplots show MOx concentration measurements and the red boxplots show LS concentration measurements. The outer edges of the enclosed areas show the lower quartile (value representing the 25th percentile of the data) and upper quartile (75th percentile) of the data. The vertical line in each box shows the median (50th percentile) of the data. The horizontal lines extending from each box show the range that encapsulates plus or minus 1.5 times the difference between the upper and lower quartile, and values exceeding this range are shown as dots. The plot is zoomed to show zero to five ppm; larger concentration measurements exist but are omitted from the plot.

3 Investigation of Meteorological Variables

MOx sensors rely on the change of resistance across the metal oxide in the sensor to produce a methane concentration estimate. This resistance is sensitive to changes in meteorological variables such as temperature and humidity. MOx sensors may also take more time to respond to increases in methane concentration since the change in resistance across the metal oxide may occur slower than the change in concentration at the sensor, so during periods of high wind speed the MOx sensors may experience systematic bias as methane is blown past the sensor faster than it can be measured. In this section we analyze how changes in temperature, humidity, and wind speed may affect the measured concentrations at the co-located MOx and LS sensors. The impact of these covariates is known to CMS technology vendors, and thus it is very likely that the vendors already employ corrections, via calibration, to adjust concentration data accordingly. Therefore, there may be small, or no, bias due to these covariates present in the data.

3.1 Temperature

We begin by analyzing the effect of temperature on the concentration difference between LS concentration measurements and MOx concentration measurements at each co-located sensor pair. We analyze the difference (LS - MOx) at the minute-level for overlapping time steps for each co-located sensor pair. Figure 3 shows the difference between LS and MOx methane concentration measurements made by co-located sensor pairs at the same time as a function of the internal temperature measured by the LS sensor.

To analyze the impact of temperature on the concentration measurement difference between the co-located LS and MOx sensors, we analyze the distribution of co-located sensor differences by five-degree Fahrenheit bins. Figure 3 shows these distributions, with each subplot showing a single co-located sensor position. The width of the boxplot represents the number of observations in each five-degree bin, with wider boxplots including more observations. We see that the median concentration difference is often greater than zero. This difference is even larger when considering concentration differences when the temperature is between 30 and 70 degrees Fahrenheit. Analyzing boxplots for the five degree bins between 30 and 70 degrees, we see that in many cases, 75%, or more, of the concentration differences are greater than zero. The difference is more pronounced at some co-located sensor positions, such as N, NW, WNW, and WSW.

Distribution of Concentration Difference by LS Sensor Internal Temperature
 Nov. 10, 2023 to Jan. 31, 2024 (Boxplot Width Represents the Number of Observations)

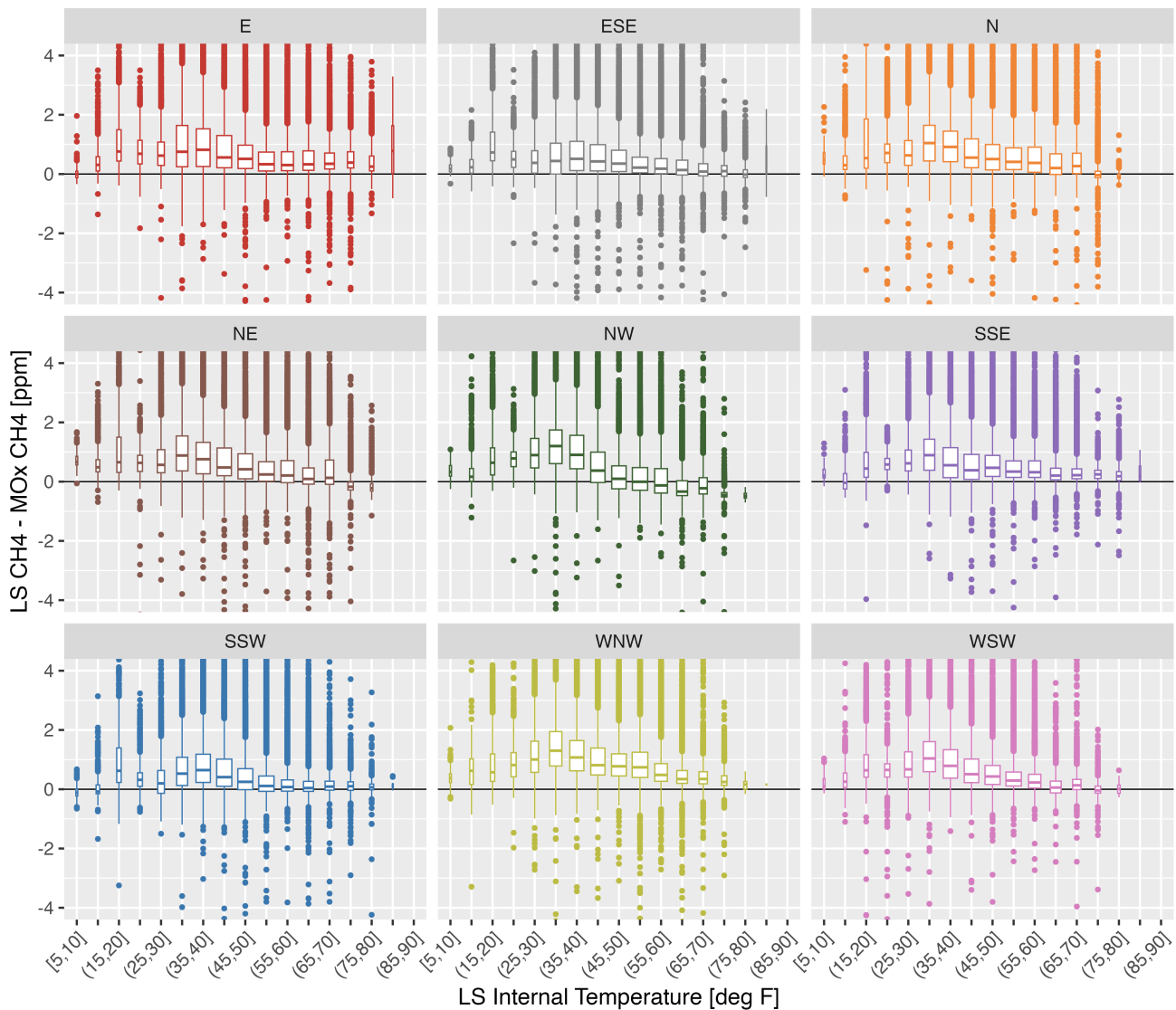


Figure 3: LS and MOx sensor concentration difference with each subplot showing a single co-located sensor location. Each boxplot shows the distribution of concentration measurement differences for a five-degree Fahrenheit bin. The width of each boxplot represents the number of observations included in each five-degree bin, with wider boxplots including more observations. A horizontal line is included showing 0 ppm difference.

3.2 Humidity

Next, we analyze the effect of humidity on the concentration difference between LS concentration measurements and MOx concentration measurements at each co-located sensor pair. Figure 4 shows the difference between co-located LS and MOx sensor concentration measurements made at the same time.

To analyze the impact that humidity has on the concentration difference between co-located LS and MOx sensor measurements taken at the same time, we analyze boxplots showing the distribution of differences by five-percent humidity bins, shown in Figure 4. With most sensor pairs, the difference between LS and MOx concentrations is positive in general for each bin, and median concentration difference values tend to increase as humidity increases.

This trend is more pronounced with certain sensor pairings, such as the WNW and WSW sensor groups. For both of these sensor groups the lower quartile concentration difference is typically greater than zero, indicating that 75% of concentration differences in each five-percent humidity bin are greater than zero. For all sensor pairings except the NW position (and only the first four bins), the LS sensor records larger concentrations than the MOx sensor, in general, in each five-percent bin.

Distribution of Concentration Difference by LS Sensor Internal Humidity
 Nov. 10, 2023 to Jan. 31, 2024 (Boxplot Width Represents the Number of Observations)

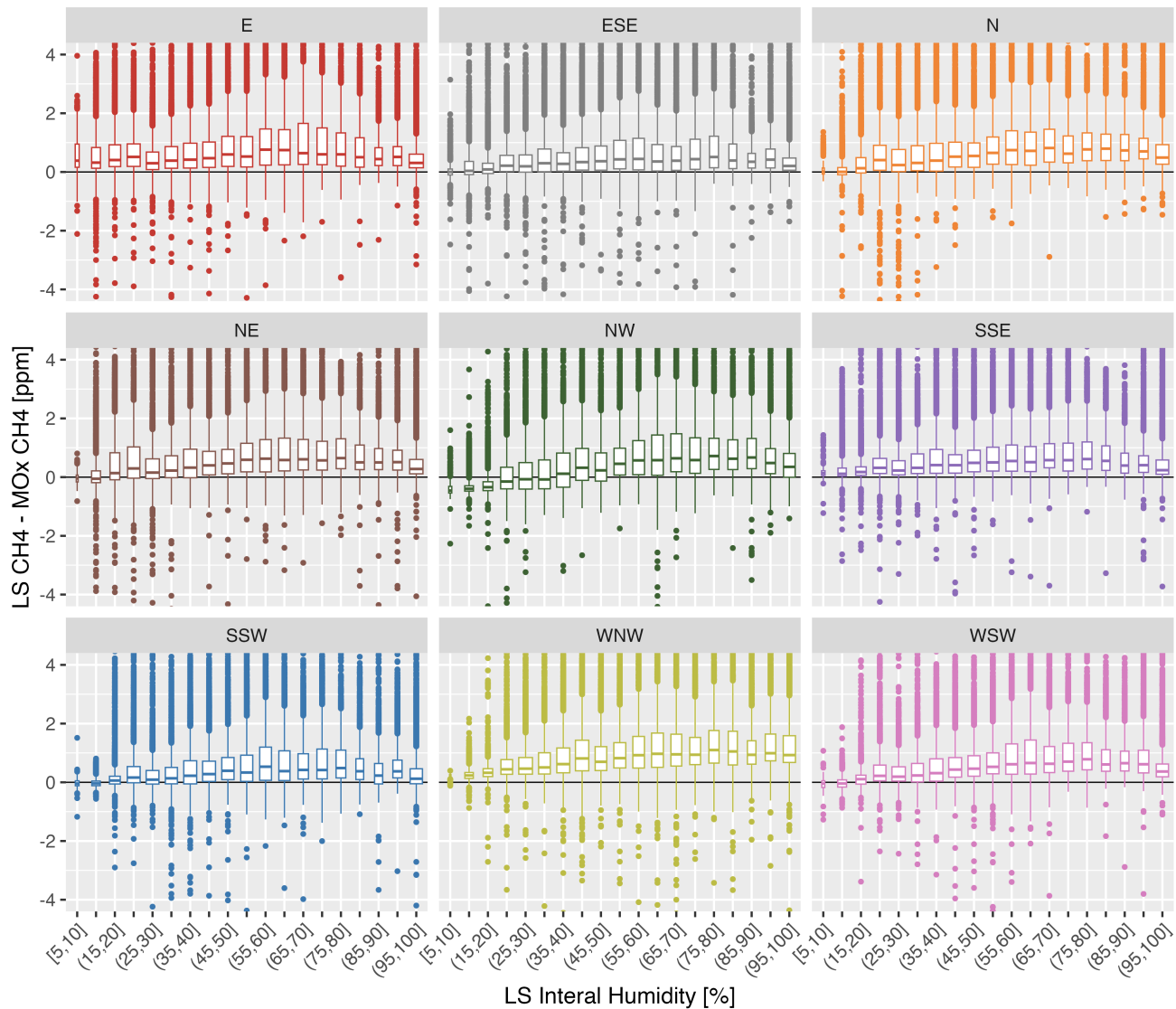


Figure 4: LS and MOx sensor concentration difference with each subplot showing a single co-located sensor location. Each boxplot shows the distribution of concentration measurement differences for a five-percent humidity bin. The width of each boxplot represents the number of observations included in each five-percent bin, with wider boxplots including more observations. A horizontal line showing 0 ppm difference is included.

3.3 Wind Speed

In this section we analyze the effect of wind speed on the concentration difference between LS concentration measurements and MOx concentration measurements at each co-located sensor pair. Figure 5 shows the

difference between LS and MOx methane concentration measurements made at co-located sensors at the same time as a function of median wind speed of all four anemometers.

To determine the impact wind speed has on co-located concentration difference for temporally aligned measurements, we examine distributions for one meter per second bins for each co-located sensor group, shown in Figure 5. We see that the LS sensors, on average, record larger concentrations than the MOx sensors, and this appears more pronounced at lower wind speeds, with a larger spread of positive concentration differences. The smaller median difference at higher wind speeds could be due to fewer observations at high wind speeds. The number of differences in each bin is shown by the width of the boxplots. In general, differences are positive, indicating that the LS sensors record larger concentrations than the MOx sensors.

Distribution of Concentration Difference by Combined Anemometer Wind Speed
 Nov. 10, 2023 to Jan. 31, 2024 Boxplot Width Represents the Number of Observations

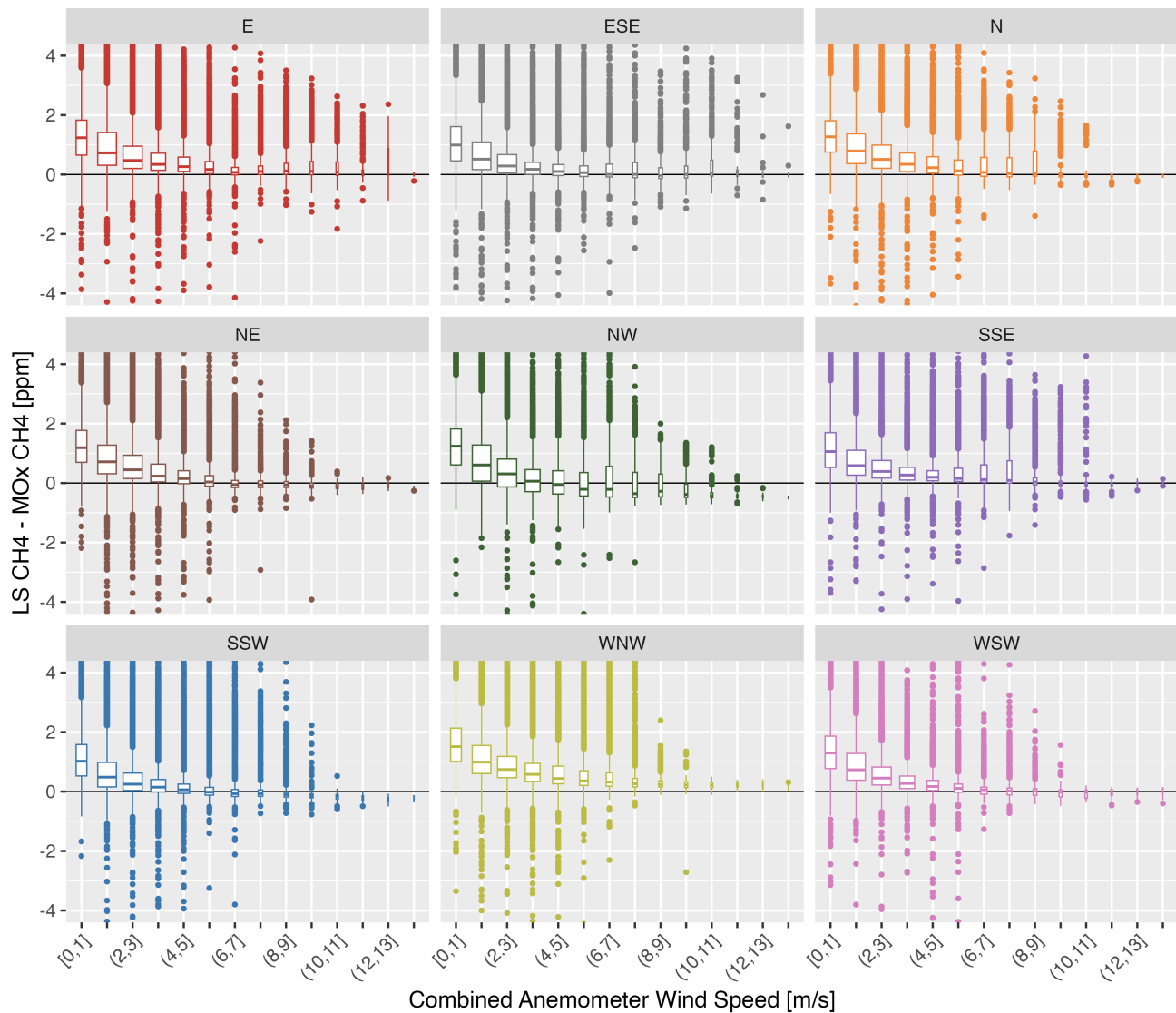


Figure 5: LS and MOx sensor concentration difference with each subplot showing a single co-located sensor location. Each boxplot shows the distribution of concentration measurement differences for a one meter per second wind speed bin. The width of each boxplot represents the number of observations included in each five-percent bin, with wider boxplots including more observations. A horizontal line showing 0 ppm difference is included.

4 Differences During Concentration Enhancements

In this section we analyze bias in just the MOx sensors during periods of enhanced methane concentrations, referred to as spikes. We treat the LS concentrations as the ground truth for this analysis as they are commonly understood to provide more accurate concentration measurements. Spikes and background are determined using the gradient-based spike detection algorithm proposed in Daniels, et. al [1]. The algorithm steps through each observation for each sensor considering the change between the current and next concentration observation. If this change is larger than a certain threshold, then this begins a spike. Once the concentration has returned to pre-spike

concentration levels, the spike is ended. In-spike concentrations are then background corrected by subtracting the concentrations measured by the sensors before and after the spike from the in-spike concentrations. Background corrected spikes with a maximum amplitude less than a certain threshold, in this case one part-per-million, are removed. The concentration time series for each sensor is passed through the spike detection algorithm and then periods of in-, and out-of-spike, concentrations can be time-matched and compared between co-located sensors. In-spike concentrations contain information about the emissions, whereas background (out-of-spike) periods just indicate that no emissions are happening. Therefore, comparing the two technologies during in-spike times is important, as these times will most directly affect any subsequent analysis (e.g., emission rate inversions). Filtering out the background times allows us to focus on the signal in which we have the most interest (the in-spike differences).

First we analyze periods where the MOx and LS sensors are both in spike, as defined by the spike detection algorithm. For these periods, we compare the average amplitude of the overlapping in-spike periods. Figure 6a shows the percent difference between temporally aligned LS and MOx spikes as a function of LS in-spike concentration quantile. As the maximum amplitude of spikes increases, the total possible difference between the MOx spike and the LS spike also increases. To account for and remove this confounding effect, we utilize percent difference to normalize for the effect of increasing difference due to increasing amplitude of spikes. We see that as the LS in-spike concentration quantile increases, the percent difference between the MOx and LS sensor in-spike concentration also increases. Figure 6b shows these distributions zoomed to -100 to 100 percent difference. For all LS in-spike concentration quantiles, the lower quartile percent difference between LS and MOx in-spike concentrations is greater than zero percent, and for LS in-spike concentration quantiles greater than 60 ppm, the median percent difference is greater than 50%. The largest percent differences are present at the largest LS in-spike concentration quantiles, indicating that as the average in-spike concentrations increase, the difference between the LS and MOx concentrations also increases, even as a proportion of the LS spike concentration.

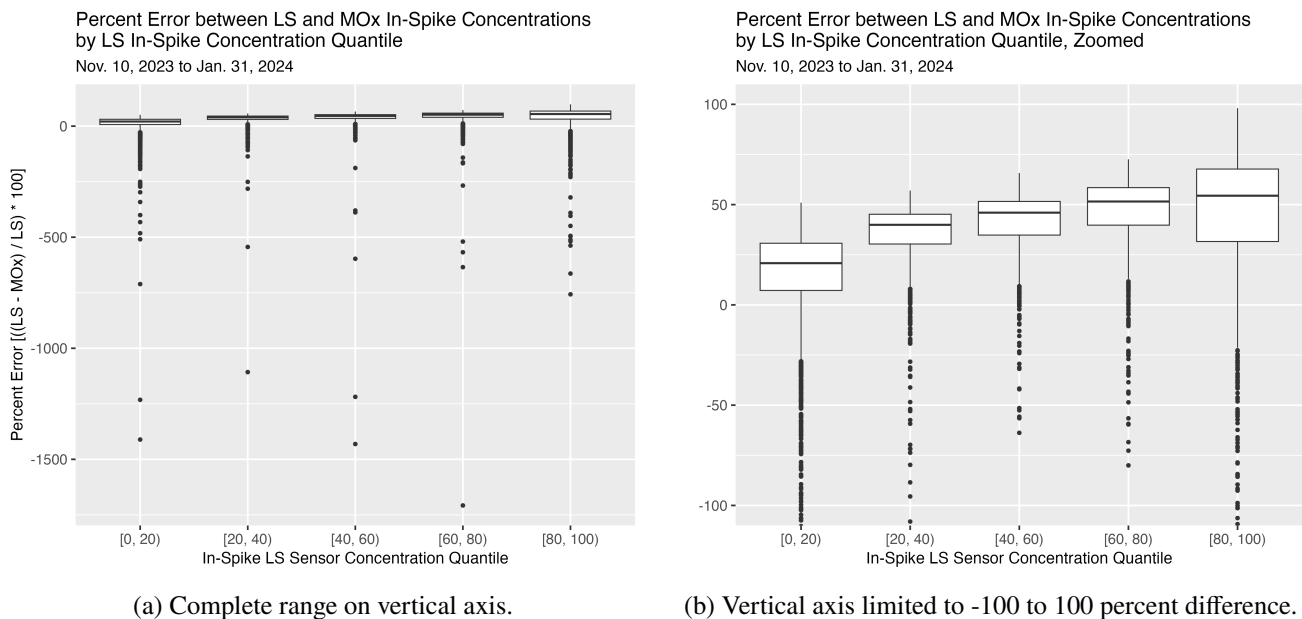


Figure 6: Distribution of percent difference between MOx and LS average in-spike amplitudes of temporally aligned spikes. Spikes are binned by the LS in-spike concentration quantile, with the largest LS spikes on the right. Positive differences indicate the LS sensor is recording larger in-spike concentrations.

We now show in-spike percent difference for each of the co-located sensor pairs. Figure 7 shows the per-pair distribution of percent difference for each 20 percentile bin of LS in-spike concentration. The overall trend seen in Figures 6a and 6b is mirrored in this plot, indicating that there is not just one sensor pair where the

difference is extreme and driving the overall trend. For all sensor pairs, as the average amplitude of the in-spike LS concentrations increases, so does the percent difference of average in-spike concentration between the LS and MOx co-located sensor pairs.

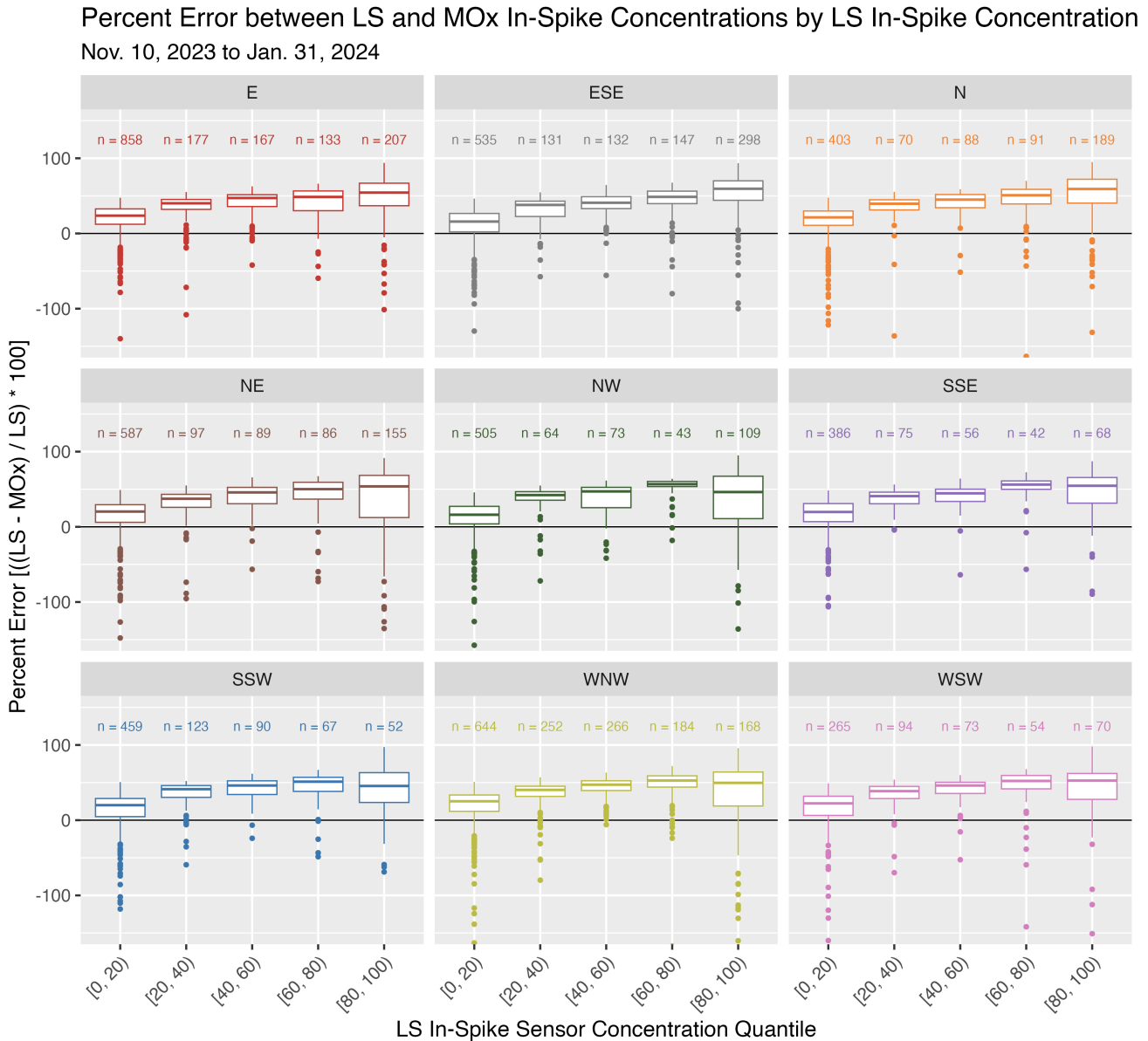


Figure 7: Distribution of percent difference between MOx and LS average in-spike amplitudes of temporally aligned spikes for each co-located sensor pair. Spikes are binned by the LS in-spike concentration quantile, with the largest LS spikes on the right. Positive differences indicate the LS sensor is recording larger in-spike concentrations. Note the vertical axis is limited to -100 to 100 percent difference.

Next we analyze the differences between in-spike and out-of-spike measurements made at the same times for the co-located sensor pairs, shown in Figure 8. First we analyze the distribution of LS and MOx concentration difference for when both co-located sensors are in a spike. This analysis is similar to that shown in Figure 6, however, we now analyze the absolute difference between LS and MOx sensors. We then analyze the difference for when only one sensor technology is in a spike: only the LS sensor in a spike, then only the MOx sensor in a spike. Finally we analyze the distribution of differences for when neither co-located sensor is in a spike,

i.e. the sensors are recording background concentrations. We analyze these different combinations as MOx and LS solutions may not record enhancements at the same time, despite being co-located. This would affect subsequent analysis (e.g., estimating emission duration), so it is important to analyze and quantify these differences.

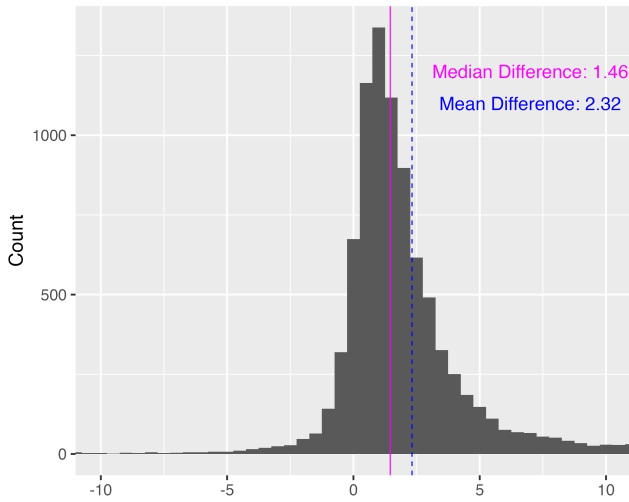
Looking first at the distribution of differences between the LS in-spike and the MOx in-spike concentrations, we see that the distribution is right skewed, with the majority of the differences being greater than zero ppm, indicating that the LS sensors, on average, record larger spike concentrations than the MOx sensors. The median difference is 1.46 ppm, and the mean difference is 2.32 ppm. Both co-located sensors are in-spike at the same time for only 2.82% of all observations.

Next we analyze the concentration difference when the LS sensor is in-spike and the MOx sensor is out-of-spike, i.e. recording site background concentrations. We see a right skewed distribution, which is expected, since the concentrations recorded during spikes in the LS sensor should be larger than the out-of-spike concentrations at the same time recorded by the co-located MOx sensor. The median concentration difference is 1.47 ppm, while the mean concentration difference is 2.54 ppm. The LS sensor is in-spike while the co-located MOx sensor is out-of-spike for 9.70% of all observations.

Next we analyze the concentration difference when the MOx sensor is in-spike, and the LS sensor is out-of-spike, i.e. recording site background concentrations. We see a left skewed distribution, which is expected, since spikes should be, on average, larger than background measurements. The median difference is -0.18 ppm, and the mean difference is -3.54 ppm. There are still differences greater than zero, indicating that the LS sensor sometimes records background concentrations that are greater than the co-located MOx in-spike concentration. The MOx sensor is in-spike while the co-located LS sensor is out-of-spike for 0.25% of the total observations. Considering previous analysis, we see that the LS sensor is in-spike while the MOx sensor is out of spike 38.8 times more often than the inverse. This likely indicates that the MOx sensors do not record many of the spikes, i.e., methane enhancements, that are occurring on the site.

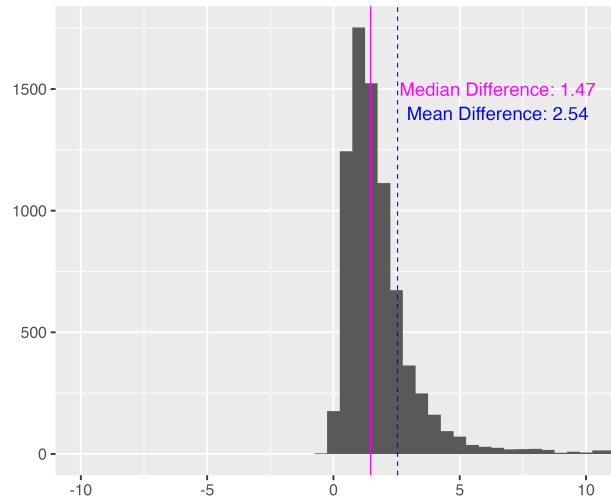
Finally we analyze the concentration difference when neither co-located sensor is recording in-spike concentrations. We see a narrow, right-skewed distribution, indicating that in general, the LS sensor records larger background concentrations than the co-located MOx sensor. The median concentration difference is 0.62 ppm, while the mean difference is 0.79 ppm. We see that neither co-located sensor records spikes for 87.24% of all observations.

Distribution of In-Spike Concentration Differences
Both In-Spike
Nov. 10, 2023 to Jan. 31, 2024



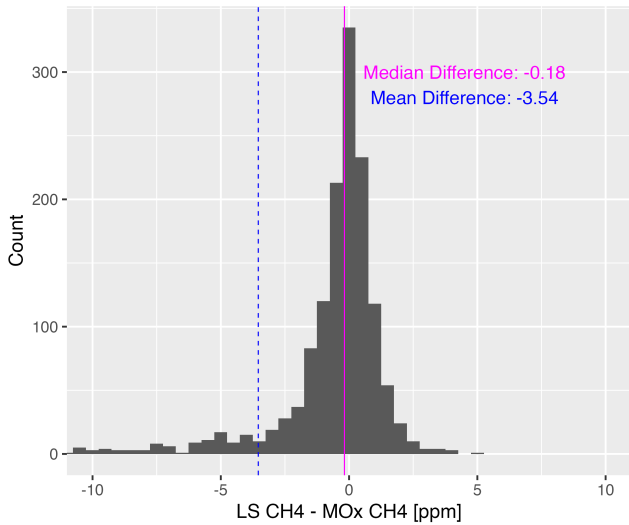
(a) Both co-located sensors in-spike.

Distribution of Concentration Differences
LS In-Spike, MOx Not
Nov. 10, 2023 to Jan. 31, 2024



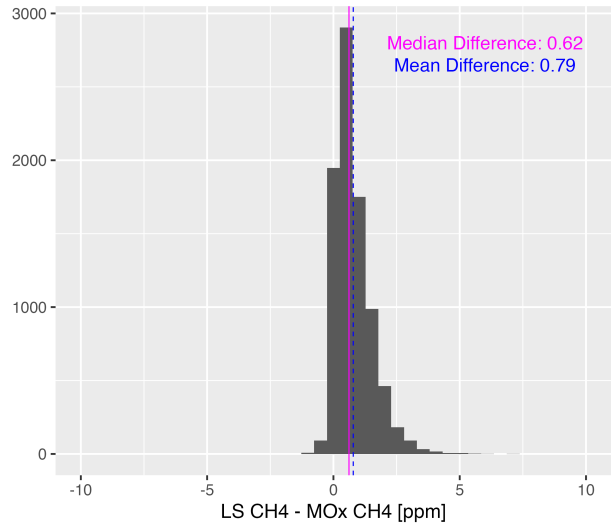
(b) LS sensor in-spike, co-located MOx sensor out-of-spike.

Distribution of Concentration Differences
MOx In-Spike, LS Not
Nov. 10, 2023 to Jan. 31, 2024



(c) MOx sensor in-spike, co-located LS sensor out-of-spike.

Distribution of Concentration Differences
Neither In-Spike
Nov. 10, 2023 to Jan. 31, 2024



(d) Both co-located sensors out-of-spike.

Figure 8: Distributions of average concentration values from co-located sensors under different regimes: both co-located sensors in-spike, one co-located sensor in-spike, and neither co-located sensor in-spike.

5 Discussion

CMS Technology vendors likely adjust the concentration readings, via calibration, that are reported to the end-user to account for different meteorological variables, such as temperature, humidity, and wind speed. When analyzing the methane concentration measurements made at the same time by the MOx and LS sensors, we find that not only do the LS sensors record larger concentrations on average, but this difference is further exacerbated by meteorological variables. The median concentration difference between the LS and MOx sensors was larger for

temperatures between 30 and 70 degrees Fahrenheit, and median concentration difference increased as a function of humidity, i.e., higher humidity led to larger median concentration difference. Finally, median concentration difference was larger at lower wind speeds, times when the MOx measurement delay should be least noticeable, and median concentration difference decreased to zero parts-per-million as wind speed increased. This could be due to the small number of observations by both sensor types at high wind speeds.

When analyzing in-spike concentration differences, the most important time periods for analysis, we found that the median percent concentration difference between LS and MOx technologies increases as the methane enhancements become larger. This is especially notable since in-spike periods give us information about when emissions are occurring on the site, whereas out-of-spike periods are when sensors are recording background concentrations. This difference implies that when concentration measurements from both sensor technologies are used in inversion algorithms to estimate emission rates, MOx sensor data would likely lead to underestimations. Further, the LS sensors recorded in-spike concentrations while the MOx sensor recorded background concentrations 38.8 times more often than the inverse, indicating that the MOx sensors often miss concentration enhancements that are detected by the LS sensors. This difference further indicates that when using concentration measurements from both sensor technologies as inputs to inversion algorithms to estimate emission rates, not only would estimated emissions rates using the MOx concentrations likely be underestimations, but emission events might be missed entirely if using the MOx concentration data. While this was not investigated explicitly in this paper, using MOx concentration data would lead likely to underestimation of fugitive, as well as operational emissions, and result in lower-than-actual emissions inventories.

References

- [1] W. S. Daniels, M. Jia, and D. M. Hammerling, “Detection, localization, and quantification of single-source methane emissions on oil and gas production sites using point-in-space continuous monitoring systems,” *Elementa: Science of the Anthropocene*, vol. 12, no. 1, p. 00 110, Mar. 2024, ISSN: 2325-1026. DOI: [10.1525/elementa.2023.00110](https://doi.org/10.1525/elementa.2023.00110). [Online]. Available: <https://doi.org/10.1525/elementa.2023.00110>.

The Payne Institute for Public Policy

AT COLORADO SCHOOL OF MINES

ABOUT THE AUTHORS

Kellis Ward

Research Scientist, Applied Mathematics and Statistics, Colorado School of Mines

Kellis Ward has his BS in Statistics and his MS in Data Science from Mines ('22, '24) and has been working with the Hammerling Research Group for just over two years. He has become an expert in inferring methane emission from continuous monitoring systems and is currently focusing on a comparative analysis of laser and metal oxide continuous monitors. Outside of research, Kellis enjoys dabbling in sports analytics, going jeeping in the San Juan mountains, and taking part in anything outdoorsy. He wants to continue with methane research since it is an essential step to helping reverse climate change and ensuring that the outdoors remains beautiful for all.

William Daniels

PhD Candidate, Applied Mathematics and Statistics, Colorado School of Mines

William Daniels is a PhD candidate in the Department of Applied Mathematics and Statistics at the Colorado School of Mines. His current research focus is on characterizing methane emissions from the oil and gas sector, including methods for emission detection and flux quantification. He is a student researcher at the Payne Institute for Public Policy and the Energy Emissions Modeling and Data Lab (EEMDL) and serves as a Core Team Member of the Methane Emissions Technology Alliance (META).

Dorit Hammerling

Associate Professor, Applied Mathematics and Statistics, Colorado School of Mines

After 8 years working in the cement industry on process and quality control, Prof. Hammerling obtained a M.A. and PhD (2012) from the University of Michigan in Statistics and Engineering developing statistical methods for large satellite data. This was followed by a post-doctoral fellowship at the Statistical Applied Mathematical Sciences Institute in the program for Statistical Inference for massive data. Prof. Hammerling subsequently joined the National Center for Atmospheric Research, where she led the statistics group within the Institute for Mathematics Applied to the Geosciences and worked in the Machine Learning division before becoming an Associate Professor in the Department of Applied Mathematics and Statistics at the Colorado School of Mines in January 2019. Prof. Hammerling received the Early Investigator Award from the American Statistical Association, Section on Statistics and the Environment, in 2018.

The Payne Institute for Public Policy

AT COLORADO SCHOOL OF MINES

ABOUT THE PAYNE INSTITUTE

The mission of the Payne Institute at Colorado School of Mines is to provide world-class scientific insights, helping to inform and shape public policy on earth resources, energy, and environment. The Institute was established with an endowment from Jim and Arlene Payne and seeks to link the strong scientific and engineering research and expertise at Mines with issues related to public policy and national security.

The Payne Institute Commentary Series offers independent insights and research on a wide range of topics related to energy, natural resources, and environmental policy. The series accommodates three categories namely: Viewpoints, Essays, and Working Papers.

For more information about the Payne Institute please visit: <https://payneinstitute.mines.edu/> or follow the Payne Institute on Twitter or LinkedIn:



DISCLAIMER: The opinions, beliefs, and viewpoints expressed in this article are solely those of the author and do not reflect the opinions, beliefs, viewpoints, or official policies of the Payne Institute or the Colorado School of Mines.